

InP and Si, whose band structures are very similar, give relatively poor behavior. The use of nonaqueous solvents have also produced several novel semiconductor effects which could not be investigated in aqueous solutions. Thus while n-InP photodecomposes in aqueous solutions (except those containing  $\text{Te}^{2-}$ ), the stability range in ACN is much larger. The extended solvent stability at negative potentials and the surface film effect allowed photoassisted electron transfer over a potential range of about twice  $E_g$ . Moreover, n- and p-type InP in ACN has recently been utilized for photoassisted electrogenerated chemiluminescence, where the irradiating red light was up-converted to violet emission (14).

#### Acknowledgment

The support of this research by the National Science Foundation and The Electrochemical Society (by an Edward Weston Fellowship to P.K.) is gratefully acknowledged.

Manuscript submitted July 5, 1978; revised manuscript received Sept. 21, 1978.

Any discussion of this paper will appear in a Discussion Section to be published in the December 1979 JOURNAL. All discussions for the December 1979 Discussion Section should be submitted by Aug. 1, 1979.

Publication costs of this article were assisted by the University of Texas at Austin.

#### REFERENCES

1. M. D. Archer, *J. Appl. Electrochem.*, **5**, 17 (1975).
2. A. B. Ellis, J. M. Bolts, and M. S. Wrighton, *This*

- Journal*, **124**, 1603 (1977).
3. A. B. Ellis, J. M. Bolts, S. W. Kaiser, and M. S. Wrighton, *J. Am. Chem. Soc.*, **99**, 2848 (1977).
4. K. C. Chang, A. Heller, B. Schwartz, S. Menezes, and B. Miller, *Science*, **196**, 1097 (1977).
5. P. A. Kohl and A. J. Bard, *This Journal*, **126**, 59 (1979).
6. P. A. Kohl and A. J. Bard, *J. Am. Chem. Soc.*, **99**, 7531 (1977).
7. D. Laser and A. J. Bard, *J. Phys. Chem.*, **80**, 459 (1976).
8. S. N. Frank and A. J. Bard, *J. Am. Chem. Soc.*, **97**, 7427 (1975).
9. (a) H. Gerischer in "Physical Chemistry: An Advanced Treatise," Vol. 9A, H. Eyring, D. Henderson, and W. Jost, Editors, Academic Press, New York (1970); (b) H. Gerischer, *Adv. Electrochem. Electrochem. Eng.*, **1**, 139 (1961).
10. P. A. Kohl, S. N. Frank, and A. J. Bard, *This Journal*, **124**, 225 (1977).
11. R. N. Noufi, P. A. Kohl, S. N. Frank, and A. J. Bard, *ibid.*, **125**, 246 (1978).
12. (a) E. C. Dutoit, R. L. Van Meirhaege, F. Cardon, and W. P. Gomes, *Ber. Bunsenges. Phys. Chem.*, **79**, 1206 (1976); (b) W. P. Gomes and F. Cardon, *ibid.*, **74**, 432 (1970); (c) R. A. L. Vanden Berghe, F. Cardon, and W. P. Gomes, *ibid.*, **77**, 290 (1973); (d) *ibid.*, **78**, 331 (1974); (e) A. M. Van Wezemael, W. H. La Fleve, F. Cardon, and W. P. Gomes, *J. Electroanal. Chem.*, **87**, 105 (1978).
13. V. A. Myamlin and Y. V. Pleskov, "Electrochemistry of Semiconductors," Plenum Press, New York (1967).
14. J. D. Luttmmer and A. J. Bard, *This Journal*, **126**, 414 (1979).

## Semiconductor Electrodes

### XVIII. Liquid Junction Photovoltaic Cells Based on n-GaAs Electrodes and Acetonitrile Solutions

Paul A. Kohl\* and Allen J. Bard\*\*

Department of Chemistry, The University of Texas at Austin, Austin, Texas 78712

#### ABSTRACT

Regenerative photoelectrochemical cells (PEC) were constructed utilizing single crystal n-GaAs in acetonitrile solutions. Solution redox couples (anthraquinone, p-benzoquinone, dimethyl ferrocene, ferrocene, hydroxymethyl ferrocene, and tetramethyl-p-phenylenediamine) whose standard redox potential varied by over 1.2V, were photooxidized at the semiconductor electrode and reduced at a Pt counterelectrode converting light directly into electrical energy. A power conversion efficiency of 14% was observed for the n-GaAs electrode in a ferrocene-ferricenium acetonitrile solution at a radiant intensity of 0.52 mW/cm<sup>2</sup> of 720-800 nm light. The efficiency and stability were found to be very dependent upon the residual water concentration, radiant power, and concentration of electroactive species.

The effective utilization of semiconductor electrodes in photoelectrochemical devices for the conversion of light energy to chemical and electrical energy depends upon a knowledge of the mechanism of charge transfer at the interface and hence of the energy level distributions within the semiconductor and solution. These determine the rates of competitive reactions of photogenerated holes or electrons and thus the stability, efficiency, and over-all electrochemical behavior of the semiconductors. The characteristics of a photoelectrochemical cell (PEC) can be predicted from the electrochemical behavior of the individual semiconductors and counterelectrode in regenerative PEC's (or liquid junction photovoltaic

cells) which show no net solution reaction and convert light to electricity, photoelectrosynthetic cells, which cause a net change in the solution composition and creation of chemical free energy (e.g., the decomposition of water to H<sub>2</sub> and O<sub>2</sub>), or in photocatalytic cells in which light is used to catalyze solution reactions at the semiconductor surface. Although a number of aqueous photovoltaic cells have been described, the recent cell by Tsubomura *et al.* (1) utilizing n-CdS and iodide ion in acetonitrile (ACN) is the only reported PEC using an aprotic solvent.

Previous studies of the electrochemical behavior of n- and p-type GaAs in anhydrous ACN solutions have shown that these semiconductors are stable under irradiation and suggested several suitable couples for use in photovoltaic PEC's (2). It was shown that:

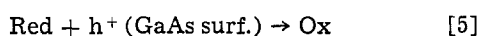
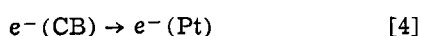
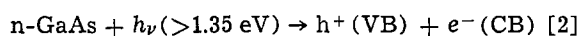
\* Electrochemical Society Student Member.  
 \*\* Electrochemical Society Active Member.  
 Key words: energy conversion, liquid photovoltaic, solar.

(i) The photodissolution of n-GaAs, which occurs at potentials positive of  $-0.7V$  vs. SCE in aqueous solutions (3), takes place in ACN only at potentials well positive of  $0V$ . This allows the use of many more redox couples spanning a large potential range. Aqueous n-GaAs PEC's (3, 4) are restricted to the use of redox couples whose standard potentials lie negative of  $-0.7V$ . (ii) Many reversible one-electron redox couples were shown to be photooxidized (on n-GaAs) at less positive or photoreduced (on p-GaAs) at less negative potentials than on platinum (i.e., show "negative overpotentials" or "underpotentials") which represents the conversion of light to electrical energy. (iii) Intermediate levels or surface states were found to mediate electron transfer between the semiconductor and solutions species and in some cases back-reactions via these levels were the limiting factors in the magnitude of the underpotential developed. The intermediate level was found to lie near the potential of photodissolution in aqueous solutions ( $\sim -0.7V$ ), which was well positive of the flatband potential ( $V_{fb}$ ). (iv) The formation of a surface film from reduction of the GaAs at potentials negative of  $V_{fb}$  was suggested; the junction between this film and the semiconductor was proposed to produce photovoltages analogous to those found at a semiconductor/metal junction which assist in electron transfer and produce underpotentials with both n- and p-GaAs. (v) The nature of the surface pretreatment (i.e., etching procedure) greatly affected the electrochemical behavior of the semiconductor.

We describe here liquid junction photovoltaic cells using n-GaAs as the semiconductor and ACN as the solvent with the general form

n-GaAs/Red ( $xM$ ), Ox ( $yM$ ), TBAP ( $0.2M$ ), ACN/Pt [1]

where Red and Ox represent soluble species in the redox couple  $Ox + e^- \rightleftharpoons Red$  and TBAP is tetra-n-butylammonium perchlorate. In all cells irradiation of the n-GaAs causes photogeneration of holes ( $h^+$ ) in the valence band (VB) and electrons ( $e^-$ ) in the conduction band (CB). The over-all cell process is thus



In these cells there is thus no over-all change in the solution composition and the total electrical energy output of the cell represents the converted light energy. The choice of redox couples was based on the previously observed electrochemical behavior in ACN (2). The cells are shown to convert low intensity light to electricity with a good efficiency and the characteristics, limitations, efficiencies and lifetimes of these cells are discussed.

### Experimental

Single crystals of n-GaAs ( $N_D = 2 \times 10^{18} \text{ cm}^{-3}$ ), obtained from Atomergic Chemicals (Long Island, New York), were provided with ohmic contacts, polished, and mounted as electrodes (areas of  $0.2\text{-}1 \text{ cm}^2$ ) as previously described (2). The semiconductors were etched prior to each use for 6 sec in 3:1:1 concentrated  $\text{H}_2\text{SO}_4$ :30%  $\text{H}_2\text{O}_2$ : $\text{H}_2\text{O}$  followed by a 25 sec etch in 6M HCl; this treatment produced the largest photocurrents and open-circuit potentials (2). The high purity ACN, electroactive compounds and supporting electrolyte, tetra-n-butylammonium perchlorate (TBAP), were all high quality materials purified, dried, and deaerated as described previously (2, 5, 6). Improved electrochemical stability was found if the

ACN was stirred with activated alumina (7) following the three vacuum distillations of the solvent over  $\text{P}_2\text{O}_5$ , as discussed below. Ferrocene and its derivatives, obtained from commercial sources, were purified as previously described (8). The chemicals were stored in an inert (helium) atmosphere glove box (Vacuum Atmospheres Corporation, Hawthorne, California); all electrochemical cells were assembled in this box. The sealed cells [as described previously (5, 6)] were fitted with an optical window for illumination, a coiled Pt wire counterelectrode separated from the main compartment by a medium porosity fritted glass disk, a second counterelectrode (area  $>20 \text{ cm}^2$ ) in the same compartment as the semiconductor electrode and multiple ground glass joint fittings for the semiconductors. The electrode in the separate compartment was used as a counterelectrode when the solution was coulometrically converted to another oxidation state.

The semiconductors were illuminated with a 450W xenon lamp (Oriental Corporation, Stamford, Connecticut) fitted with a water jacketed red filter. A grating monochromator (blazed at  $1 \mu\text{m}$ ), 60 nm band pass filter and 720 and 800 nm cut off filters were used for wavelength selection. The incident radiant power was measured with a Model 550-1 Radiometer/Photometer (E.G. & G., Salem, Massachusetts).

The electrochemical experiments were performed with a PAR 173 potentiostat (Princeton Applied Research, Princeton, New Jersey). The current-voltage output curves of the PEC's were obtained either by (i) measuring the voltage across a variable resistor in series with the two electrodes, or (ii) applying a variable voltage of opposite polarity to that produced by the cell and measuring the current simultaneously with the voltage. The two methods gave identical results.

In some cases, as noted, the light intensity at the electrode surface was obtained from that incident on the cell by correcting for the solution absorbance, measured with a Cary Model 14 spectrophotometer.

### Results and Discussion

The construction of the PEC's and selection of the redox couples followed directly from the electrochemical behavior found for n-GaAs in acetonitrile (2). To demonstrate the previously described ability for energy conversion of the nonaqueous n-GaAs systems, redox couples whose standard potentials ( $E^\circ$ ) spanned a range of over 1.2V were used. The power efficiencies were generally measured using light of a wavelength which was not absorbed by the solution species. In most cases, only minor corrections were made for the solution absorption as noted. The characteristics of the different PEC's are summarized in Table I and are discussed in more detail below. The relative error in efficiencies mainly reflects the uncertainty in measurement of the radiant power.

**TMPD-TMPD<sup>+</sup> cells.**—Several cells with Ox = TMPD<sup>+</sup> and Red = TMPD (Eq. [1]) were constructed. A cell current vs. potential curve for a solution in which  $x = 46 \text{ mM}$  and  $y = 0.12 \text{ mM}$  is shown in Fig. 1a. The curve represents irradiation with light of 720-800 nm by subtracting the current and power of the 800 nm cut off filter from the 720 nm filter. The short-circuit photocurrent was directly proportional to the radiant intensity. With an input power of  $0.45 \text{ mW/cm}^2$ , the maximum output power occurred at  $0.31V$  and  $148 \mu\text{A/cm}^2$  yielding an output power of  $46 \mu\text{W/cm}^2$  and  $10.2(\pm 0.5)\%$  conversion of light to electricity. After passage of 22C of charge through the external circuit (representing a turnover of the TMPD<sup>+</sup> of 76) a slight decrease in the TMPD<sup>+</sup> concentration was noticed; this is probably attributed to a slight instability of the radical cation and not to

Table I. Output parameters for the cells of the form n-GaAs/Red(xmM), OX(ymM), TBAP(0.2M), ACN/Pt\*

Redox couple*	[Red], x (mM)	[Ox], y (mM)	Light intensity (mW/cm <sup>2</sup> )	$\lambda$ (nm)	Cell voltage (V)	Cell current density (mA/cm <sup>2</sup> )	Maximum power efficiency (%)
TMPD	46	0.12	0.46	720-800	0.31	0.148	10.2
TMPD	46	0.12	10.6	720-800	0.35	2.00	6.6
TMPD	46	0.12	0.1	720-800	0.2	0.020	4
Ferrocene	104	0.82	0.52	720-800	0.375	0.195	14†
Ferrocene	104	0.82	2.4	720-800	0.35	0.925	13.4†
Ferrocene	104	0.82	5.6	720-800	0.35	1.675	9†
	104	0.8	75	Solar spectrum	0.2	9.000	2.4
Dimethyl ferrocene	140	0.7	0.414	720-800	0.33	0.125	10.9†
Hydroxymethyl ferrocene	15.7	0.83	0.24	720-800	0.25	0.080	8.3†
Hydroxymethyl ferrocene	15.7	0.83	0.45	720-800	0.27	0.137	8.2†
Anthraquinone	3	2.5	2	600-1000	0.28	0.600	8.4†
p-Benzoquinone	10	10	0.096	600	0.40	0.028	11.6†

\* Abbreviations used in this table: TBAP, tetra-n-butylammonium perchlorate; TMPD, N,N,N',N'-tetramethyl-p-phenylenediamine.

† Corrected for solution absorbance.

any dissolution of the GaAs. During such an extended trial the GaAs showed neither an apparent change in weight ( $<1 \text{ mg/cm}^2$ )<sup>1</sup> nor a change in the surface appearance. During the trial the blue radical cation was observed streaming from the GaAs surface. In reporting the efficiency no corrections were made for light absorption by TMPD<sup>+</sup> or other solution components or for reflection.

The cell performance can best be understood by considering the current-potential (*i*-*V*) curves of the electrodes and the different current components which contribute to the over-all semiconductor current. A plot of the partial currents in this PEC at two different irradiation intensities are shown in Fig. 2. The partial current for the photooxidation of TMPD via

<sup>1</sup> Since a weight change of 0.1 mg is equivalent to  $\sim 4C$  going to a dissolution reaction of GaAs (assuming  $n = 6$ ), this is not a very sensitive test of semiconductor stability. More extensive tests would be required to demonstrate very long-term stability of the material.

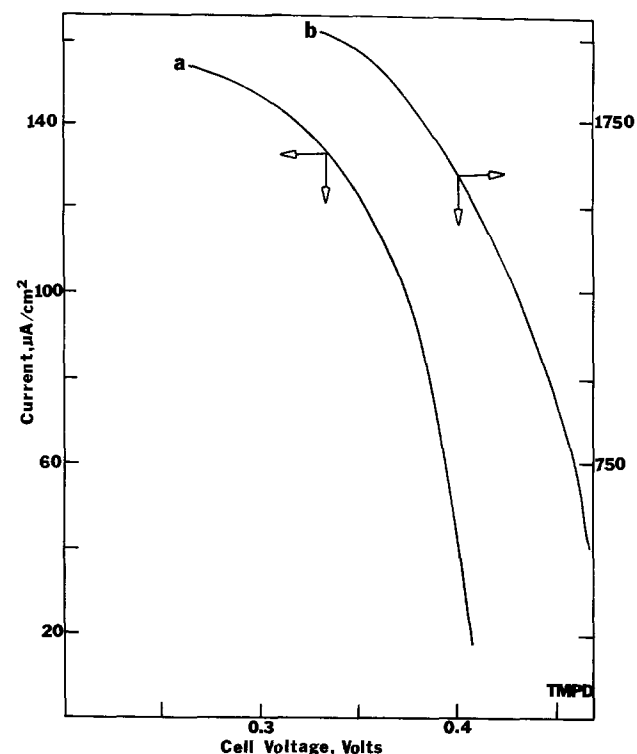
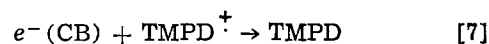


Fig. 1. Current vs. cell voltage for the cell

n-GaAs/TMPD(46 mM), TMPD<sup>+</sup> (0.12 mM), TBAP (0.2M)ACN/Pt illuminated with 720-800 nm light of intensity (a) 0.45 mW/cm<sup>2</sup> and (b) 10.6 mW/cm<sup>2</sup>.

photogenerated holes in the absence of TMPD<sup>+</sup> occurs at potentials just positive of  $V_{fb}$  ( $-1V$ ) (Fig. 2a).

However, the back reaction, i.e., reduction of TMPD<sup>+</sup> (Eq. [7])



occurred at potentials positive of  $V_{fb}$  (via an intermediate level mechanism (2)) as shown by curves b and c

for two different concentrations of TMPD<sup>+</sup>. The overall GaAs current results from a combination of these partial currents and leads to no net current at potentials negative of  $-0.6V$  vs. SCE. At less negative potentials the rate of reduction of TMPD<sup>+</sup> decreases and

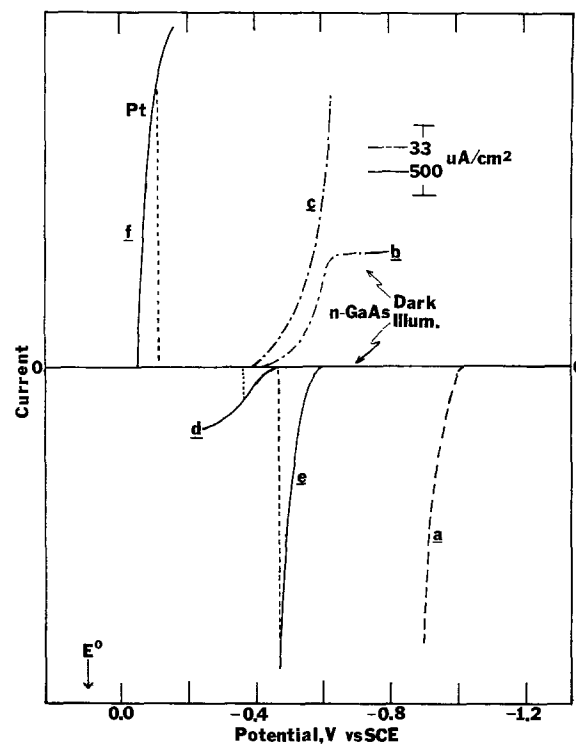


Fig. 2. Current-potential curves for (a) n-GaAs photoanode in absence of back reaction, (b) reduction of 0.12 mM TMPD<sup>+</sup> solution on n-GaAs in the dark, (c) reduction of 0.6 mM TMPD<sup>+</sup> solution, (d) photooxidation of 46 mM TMPD solution with 1.28 mW/cm<sup>2</sup> of 720-800 nm light, (e) same as (d) but with 10.6 mW/cm<sup>2</sup> light, and (f) reduction of 46 mM TMPD, 0.12 mM TMPD<sup>+</sup> solution at a Pt electrode of  $>20 \text{ cm}^2$ .

a net photoanodic current results; thus combination of curves b or c with curve a yields the net GaAs current given by curves d or e for two different light intensities. The net cell behavior, as shown in Fig. 1 and Table I, is obtained by combining the net GaAs curves (2d or e) with the Pt counterelectrode curve (2f).

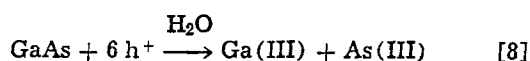
Although only a few attempts were made to maximize the power efficiency by varying the concentration of TMPD,  $\text{TMPD}^+$ ,  $\text{H}_2\text{O}$ , and lamp intensity, a few general trends in cell design were noticed. (i) Mass transfer controlled supply of reactant (i.e., concentration polarization) at either electrode limited the current and decreased the efficiency. Concentration polarization at the n-GaAs was avoided by maintaining a sufficiently high TMPD concentration and stirring rate so that the flux of TMPD to the electrode was higher than the flux of holes to the surface. The

small concentration of  $\text{TMPD}^+$  at the counterelectrode was counterbalanced by using a large area Pt electrode. When the original cell was irradiated with a light intensity of  $10.6 \text{ mW/cm}^2$ , a maximum power of 6.6% was observed at a steady-state current of  $2 \text{ mA/cm}^2$  at  $0.35\text{V}$  (Fig. 1b). Although the cell potential was higher at this intensity, the current appeared to be limited by the rate of mass transfer of  $\text{TMPD}^+$  to the Pt electrode. (ii) The back reaction

(i.e., reduction of  $\text{TMPD}^+$ ) on n-GaAs limited the output voltage and current. At larger cell voltages the relative current is smaller at higher concentrations of

$\text{TMPD}^+$  because of the back reaction (Fig. 2c vs. 2b). Similarly at lower light intensities the back reaction has a greater effect (Fig. 2d vs. 2e). Thus, lower light

intensities or high concentrations of  $\text{TMPD}^+$  do not produce as high efficiencies, because at larger voltages the photon flux must first compensate for the reduction current of  $\text{TMPD}^+$  at n-GaAs before a net oxidation is observed. When the light intensity was decreased to  $100 \mu\text{W/cm}^2$ , a maximum efficiency of 4% was found ( $20 \mu\text{A/cm}^2$  at  $0.2\text{V}$ ). (iii) The residual water concentration had a large effect on the efficiency and lifetime of the system. In aqueous solutions the GaAs undergoes photodissolution at potentials positive of  $-0.7\text{V}$  (Eq. [8]) so that operation with the GaAs at the potentials used here ( $+0.1$  to  $-0.6\text{V}$  vs.



SCE) would not be possible in aqueous media.

The occurrence of even a small amount of lattice oxidation because of small amounts of water in the ACN appeared to passivate the GaAs and thus destroy the photovoltaic effect. As shown previously in cyclic voltammetric experiments (2), when the flux of holes exceeded the flux of TMPD, the current and underpotential decayed on subsequent potential scans. After injection of  $0.5 \text{ ml}$  of  $\text{H}_2\text{O}$  into  $25 \text{ ml}$  of the original cell solution, the current decayed to 25% of its initial value after  $0.05\text{C}$  had passed. The lifetime and efficiency of the original cell depended on the radiant intensity relative to the water concentration. When the original cell was operated at  $-0.31\text{V}$  and  $150 \mu\text{A/cm}^2$ , a 2% increase in current was observed after 21 hr. However, when the intensity was increased so that the cell current was  $360 \mu\text{A/cm}^2$ , the current decayed continuously, as shown in Fig. 3. This was attributed to a more successful competition of the passivation process for holes at higher light intensities and current densities. (iv) The absorption of light by the solution was minimized by keeping the concentration of the colored species,  $\text{TMPD}^+$ , low. (v) Surface pre-

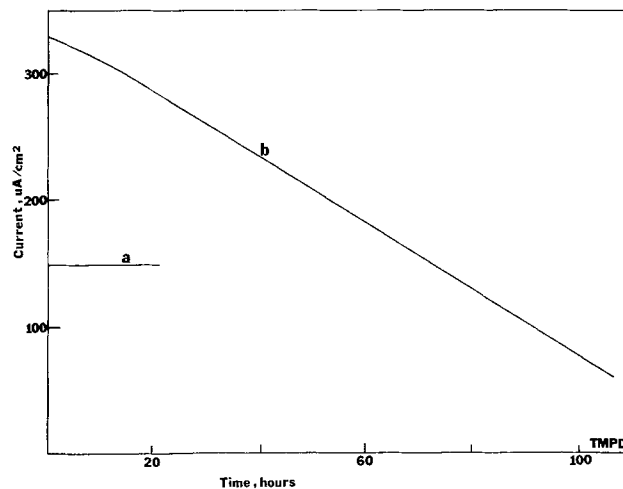


Fig. 3. Cell current vs. time for two different light intensities where that of (b) is 2.2 times that cell as in Fig. 1.

treatments, as discussed previously (2) and as will be illustrated in a later example, greatly affected the magnitude of the photocurrent and efficiency.

**Ferrocene-ferricenium cells.**—Wrighton and co-workers (9) have demonstrated that the ferrocene-ferricenium couple was useful in stabilizing Si photoanodes in PEC's with ethanolic solutions. The characteristics of such a cell with n-GaAs and ACN solutions of this couple are illustrated in Fig. 4a. When the light intensity at the GaAs surface is calculated by correcting that incident on the cell ( $0.52 \text{ mW/cm}^2$ ) using the solution absorptivity of 0.082 (6 mm of solution), a maximum power conversion efficiency of  $14 (\pm 1)\%$  was observed (output current density  $195 \mu\text{A/cm}^2$  at  $0.375\text{V}$ ). With solar radiation ( $75 \text{ mW/cm}^2$ ) this cell produced an open-circuit photopotential of  $580 \text{ mV}$  and a current of  $9 \text{ mA/cm}^2$  at  $0.2\text{V}$ , for a solar power conversion of 2.4%.

The lifetime of the cells again depended upon the residual water concentration. The behavior of the cell described above in which the ACN was triply distilled over  $\text{P}_2\text{O}_5$  is shown in Fig. 4b, curve 1. A more complete removal of water by 30 hr of stirring of the ACN containing the ferrocene and TBAP over alumina greatly improved the stability as shown by curve 2. Injection of  $500 \mu\text{l}$  of  $\text{H}_2\text{O}$  into the solution (25 ml) caused the cell current to decay to almost zero in a relatively short period of time because of the passivation of the n-GaAs. Decomposition of the adhesives and electrode supports prevented experimental trials with durations of longer than several days. During such trials there was no visual deterioration or weight loss ( $< 1 \text{ mg/cm}^2$ ) caused by photodissolution of the n-GaAs.

The electrochemical behavior of the 1,1-dimethylferrocene redox couple was very similar to that observed with  $\text{TMPD}^+$  and ferrocene. With cyclic voltammetry at an n-GaAs electrode, as described in (2), the reduction of the dimethylferrocene cation in the dark was observed on n-GaAs at potentials well negative of the  $E^\circ$  of the dimethylferrocene redox couple as determined with a Pt microelectrode, as shown in Fig. 5. When illuminated with light of energy greater than the bandgap, an underpotential of  $\sim 0.6\text{V}$  was observed for the oxidation. Upon scan reversal, after positive going scans in the light, the reduction peak height increased, because the concentration of the cation, which was photogenerated at the electrode surface, was higher. This reduction of the cation represents the back reaction in a PEC which must be minimized for efficient operation while still maintaining an adequate flux of the cation at the counterelectrode. As shown in Table I conversion

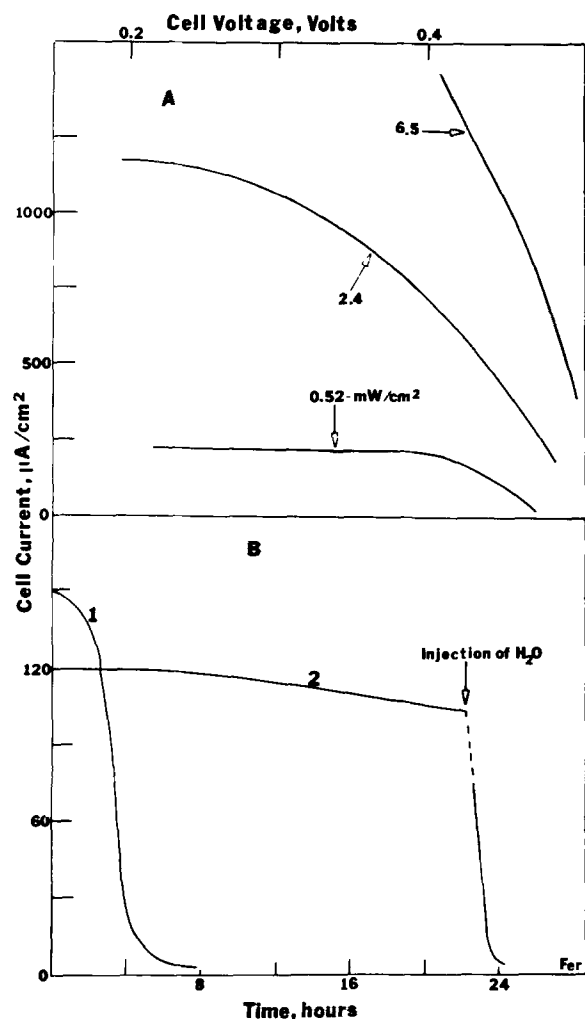


Fig. 4. (a) Cell current vs. potential for three different intensities of 720-800 nm light for the cell n-GaAs/ferrocene(0.108M), ferricenium(0.87 mM), TBAP(0.2M)ACN/Pt (b) Cell current vs. time (1) cell as in part (a); (2) [ferrocene] = 0.146M and [ferricenium] = 2.4 mM. 500  $\mu$ l of water injected in the cell as indicated.

efficiency greater than 10% was observed with the cell producing the  $i$ - $V$  curves given in Fig. 6.

The  $i$ - $V$  curves for a PEC containing the hydroxymethyl ferrocene couple as described in Table I, are given in Fig. 7. The reported efficiency is based on an incident light intensity corrected for solution absorption. Increasing the cation concentration to about 2 mM decreased the power efficiency to about 6.5%, probably because of the increased rate of the back reaction. The cell current vs. time curves were similar to those for ferrocene (Fig. 4b, curve 2) and again there was no apparent change in weight or appearance of the electrode after about 24 C/cm<sup>2</sup> of charge was passed.

**Quinone cells.**—The limited solubility of AQ allowed only rather dilute solutions to be used as shown in Table I. An open-circuit photovoltage of 700 mV was observed with the AQ cell at higher light intensities. As noted previously (2), the largest and most efficient photocurrents were observed after the GaAs was first biased to potentials more negative than  $-2V$  vs. SCE, presumably because of the development of a surface layer. The surface pretreatment also greatly affected the cell output and over-all electrochemical behavior of the n-GaAs. When the electrode was etched in only HCl without the H<sub>2</sub>SO<sub>4</sub>:H<sub>2</sub>O<sub>2</sub>:H<sub>2</sub>O etchant, a much smaller photocurrent was observed under similar conditions. The

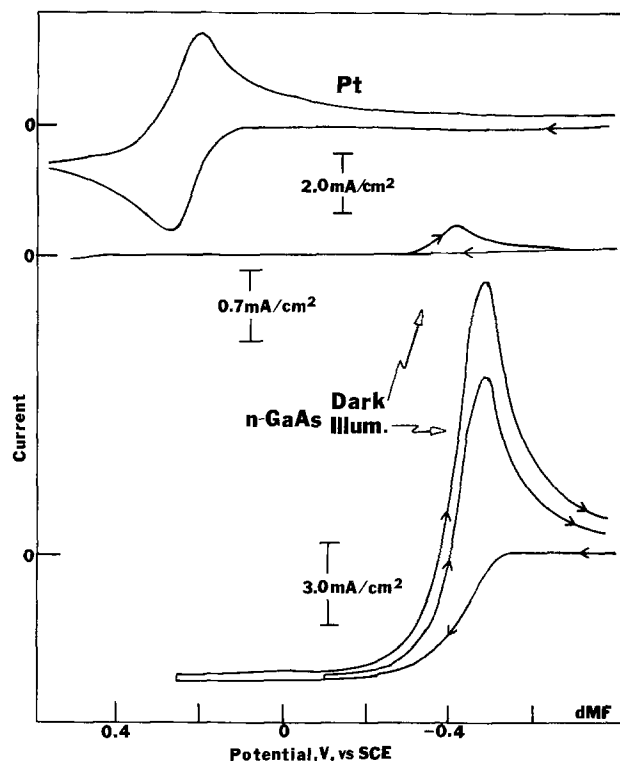


Fig. 5. Cyclic voltammogram of (a) 6.1 mM solution of dimethyl ferrocene at a Pt disk electrode, (b) and (c) 140 mM dimethyl ferrocene, 0.7 mM dimethyl ferricenium at a single crystal n-GaAs electrode in the dark and illuminated with red light. The scan rate was 0.2 V/sec and the supporting electrolyte was 0.2M TBAP.

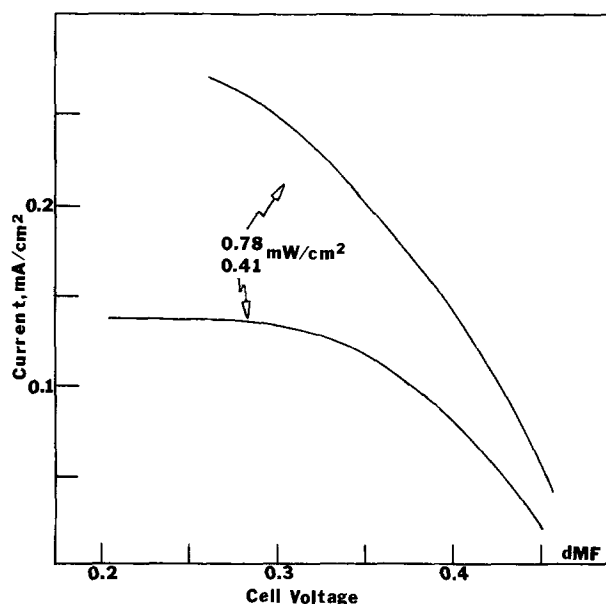


Fig. 6. Cell current vs. voltage for two intensities of 720-800 nm light for the cell n-GaAs/dimethyl ferrocene (0.14M), dimethyl ferricenium (0.7 mM), TBAP (0.2M) ACN/Pt

p-n cell utilizing both p- and n-GaAs

p-GaAs/AQ(2.5 mM), AQ<sup>-</sup> (3 mM),

TBAP(0.1M)ACN/n-GaAs [9]

produced an open-circuit photovoltage ( $V_{oc}$ ) of 920 mV. This high value for  $V_{oc}$  can be attributed to underpotentials developed at both electrodes when both are irradiated. A high (corrected) efficiency was found with a PEC utilizing BQ and its radical anion (Table

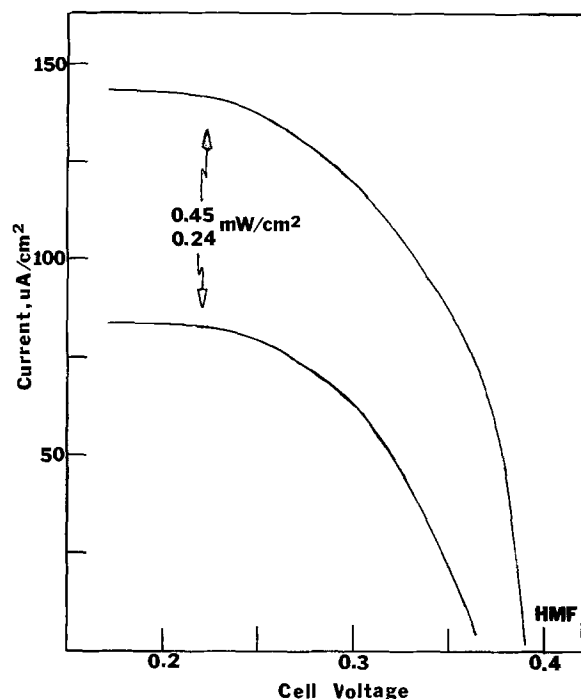


Fig. 7. Cell current vs. voltage for two intensities of 720-800 nm light for the cell n-GaAs/hydroxymethyl ferrocene (15.7 mM), hydroxymethyl ferricenium (0.83 mM), TBAP (0.2M), ACN/Pt

I) when irradiated with 600 nm light through a filter (10 nm band pass).

In general, there was no evidence of photodissolution of the GaAs in any of the cells. The wide potential range of electrochemical stability, and hence the large numbers of redox couples which can be used in the PEC's, is possible only in nonaqueous solvents where the extent of the photodissolution reaction is decreased and surface effects can produce photovoltages over a large potential range. Although reasonable efficiencies are demonstrated, the maximum efficiency appears to be a compromise of several factors hinging on the light intensity, water concentra-

tion, counterelectrode area, and the concentration of the reduced and oxidized species. The cells presented represent only a crude attempt to demonstrate the factors involved in simple regenerative PEC's. Although nonaqueous systems suffer from a number of disadvantages compared to aqueous ones, such as generally lower solubilities of (usually colored) solution redox couples and higher solution resistances, the main advantage of GaAs in ACN appears to be its wide potential range for PEC's of not only the regenerative form but also for photoelectrosynthesis and photocatalysis.

#### Acknowledgment

The support of this research by the National Science Foundation, Robert A. Welch Foundation, and The Electrochemical Society's Edward Weston Fellowship (P.K.) is gratefully acknowledged. The interest and assistance of Rommel N. Noufi is also gratefully acknowledged.

Manuscript submitted July 11, 1978; revised manuscript received Sept. 21, 1978.

Any discussion of this paper will appear in a Discussion Section to be published in the December 1979 JOURNAL. All discussions for the December 1979 Discussion Section should be submitted by Aug. 1, 1979.

Publication costs of this article were assisted by The University of Texas at Austin.

#### REFERENCES

1. K. Nakatani, S. Matsudaiva, and H. Tsubomura, *This Journal*, **125**, 406 (1978).
2. P. A. Kohl and A. J. Bard, *This Journal*, **126**, 59 (1979).
3. A. B. Ellis, J. M. Bolts, S. W. Kaiser, and M. S. Wrighton, *J. Am. Chem. Soc.*, **99**, 2848 (1977).
4. K. C. Chang, A. Heller, B. Schwartz, S. Menezes, and B. Miller, *Science*, **196**, 1097 (1977).
5. P. A. Kohl and A. J. Bard, *J. Am. Chem. Soc.*, **99**, 7531 (1977).
6. S. N. Frank and A. J. Bard, *ibid.*, **97**, 7427 (1975).
7. O. Hammerich and V. D. Parker, *Electrochim. Acta.*, **18**, 537 (1973).
8. J. R. Pladziewicz and J. H. Espenson, *J. Am. Chem. Soc.*, **95**, 56 (1973).
9. K. D. Legg, A. B. Ellis, J. M. Bolts, and M. S. Wrighton, *Proc. Nat. Acad. Sci., USA*, **74**, 4116 (1977).

## Electrochemical Potential Spectroscopy: A New Electrochemical Measurement

A. H. Thompson\*

Exxon Research and Engineering Company, Corporate Research Laboratories, Linden, New Jersey 07936

#### ABSTRACT

A new electrochemical technique is described that involves applying a series of constant potential steps to an electrochemical cell. On each potential step the cell is permitted to attain quasi open-circuit conditions by letting the current decay to a small, but finite, value. When small voltage steps are made, the voltage-charge relation is a highly precise and accurate approximation to the thermodynamic properties of the cell. Application to the Li-TiS<sub>2</sub> couple shows that the charge accumulated on each voltage step resembles an electrochemical potential spectrogram that provides evidence for the structural ordering of lithium in Li<sub>x</sub>TiS<sub>2</sub>. The technique may be used to study the potential-dependent cell kinetics, the thermodynamics of adsorption on surfaces, and the phase diagrams of cathode materials.

Recent reports (1, 2) have shown that high energy density lithium batteries can be based on the inter-

calation reaction in layered compounds. In these cells the cathode is comprised of a compound with a layered structure such as TiS<sub>2</sub>, the anode is an alkali metal (typically lithium), and the electrolyte is based on

\* Electrochemical Society Active Member.  
Key words: battery, alkali, metal, graphite, intercalation.